10

Characteristic properties of ceramics luminescence based on cubic $(ZR_{0.82-x}HF_xY_{0.17}Eu_{0.01})O_{1.91}$

© A.A. Shakirova, E.V. Dementeva, T.B. Popova, M.V. Zamoryanskaya

Ioffe Institute, St. Petersburg, Russia

e-mail: azaliya.s@inbox.ru

Received November 23, 2022
Revised March 20, 2023
Accepted March 21, 2023.

The ceramics based on cubic $(Zr_{0.82-x}Hf_xY_{0.17}Eu_{0.01})O_{1.91}$ with different contents of hafnium were studied. In the work, the elemental composition of the samples was obtained, the cathodoluminescence (CL) spectra and decay kinetics of europium luminescence were studied. The researched showed increase in the content of hafnium doesn't affect the position and number of observed bands in the luminescence spectrum. The electric dipole and magnetic dipole radiative transitions ratio was estimated for all samples. It's demonstrated that a decrease in the local symmetry of the europium ion associated with an increase in the hafnium content. It's shown the $^5D_0-^7F_1$ transition Eu^{3+} decay time doesn't depend on the hafnium content, but varies significantly in different regions of the sample, which can be attributed to the influence of grain boundaries.

Keywords: $(Zr,Hf,Y,Eu)O_2$ solid solution, cathodoluminescence, asymmetry coefficient, luminescence decay kinetics.

DOI: 10.61011/EOS.2023.05.56509.76-22

Introduction

Recently, important tasks of dosimetry are associated with the disposal and immobilization of nuclear waste, analysis of the consequences of large-scale radiation accidents and environmental disasters. Thermoluminescence dosimeters are widely used for these purposes. A essential step is the development of radiation-resistant thermoluminescence dosimeters capable of measuring high doses of ionizing radiation [1].

One of the potential materials for creating radiation-chemically resistant dosimeters is ceramics based on cubic stabilized zirconium oxide. Such a material has high mechanical, chemical and radiation resistance [2], however, the f-ZrO_2 cubic phase is unstable at room temperature, to stabilize it, rare-earth ion oxide R_2O_3, for example Y_2O_3 [3].

One of the disadvantages of zirconium is that it is transparent to neutrons, which can lead to significant energy loss when detecting high energy radiation. The chemical analogue of zirconium — hafnium, in turn, absorbs neutrons well, and its addition will allow to obtain a material capable of absorbing neutrons and having a high radiation resistance [4].

Trivalent europium ions [5] are often used to activate oxide matrices. In addition to the fact that Eu^{3+} has bright luminescence in the red area of the spectrum, it also allows to study the structural features of wide-band materials. In some cases, an analysis of the shape of the emitted spectrum of Eu3+ allows to estimate the local environment of this ion and, consequently, the symmetry of the matrix in which it is included [6].

The purpose of this paper — is to study the effect of hafnium content on cathodoluminescent properties.

Samples and methods of investigation

In this paper, we studied a concentration series of ceramic samples based on cubic zirconia $(Zr_{0.82-x}Hf_xY_{0.17}Eu_{0.01})O_{1.91}$ with different hafnium content ($x = 0$, 0.41, 0.62, and 0.82):

sample 0-Hf $(Zr_{0.82}Y_{0.17}Eu_{0.01})O_{1.91}$;
sample 0.41-Hf $(Zr_{0.41}Hf_{0.41}Y_{0.17}Eu_{0.01})O_{1.91}$;
sample 0.62-Hf $(Zr_{0.2}Hf_{0.62}Y_{0.17}Eu_{0.01})O_{1.91}$;
sample 0.82-Hf $(Hf_{0.82}Y_{0.17}Eu_{0.01})O_{1.91}$.

According to the literature data, the content of yttrium is 0.17 form. units is sufficient to stabilize the cubic phase of zirconium oxide [3], and when the content of europium is 0.01 form. units, there is the brightest luminescence [7].

The samples were synthesized by coprecipitation from a common aqueous solution followed by cold pressing and annealing in air at a temperature of 1500°C for 3 h (the synthesis is described in detail in the papers [8,9]). The characteristic grain size for this ceramic is $2-6\,\mu$m. The samples were ground and polished, and a carbon film was applied to their surface to ensure electrical conductivity.

The elemental composition of the studied samples was determined by electron microprobe analysis (EMPA). The study of the composition was carried out on a CAMEBAX electron probe microanalyzer equipped with four X-ray spectrometers with the following electron beam parameters: energy $U = 20$ keV, absorbed current $I = 15$ nA, beam diameter $d = 2\,\mu$m. For analysis, the analytical line Lα was chosen for all elements. Metallic zirconium (for Zr),

Table 1. Elemental composition of samples

Sample	Content of elements, form. un			
	Hf	Zr	Y	Eu
0-Hf	0	0.80 ± 0.02	0.185 ± 0.004	0.012 ± 0.001
0.41-Hf	0.40 ± 0.01	0.40 ± 0.01	0.187 ± 0.004	0.013 ± 0.001
0.62-Hf	0.61 ± 0.01	0.186 ± 0.004	0.194 ± 0.004	0.014 ± 0.001
0.82-Hf	0.78 ± 0.02	0	0.207 ± 0.004	0.012 ± 0.001

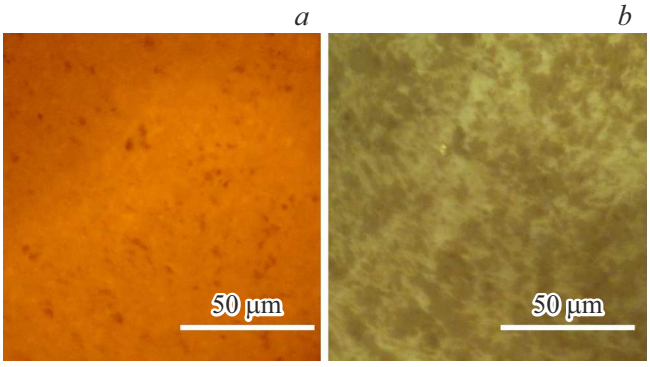

Figure 1. (*a*) CL sample image; (*b*) image of a sample in an optical microscope.

metallic hafnium (for Hf), compounds $Y_3Al_5O_{12}$ (for Y) and $EuPO_4$ (for Eu) were selected as standards. The oxygen content was calculated based on stoichiometry. The elemental composition was measured in several (minimum five) randomly selected areas of the samples and then averaged.

The luminescent properties of a concentration series of samples were studied by cathodoluminescence (CL) using the same CAMEBAX setup, additionally equipped with an optical spectrometer [10]. The CL spectra and the decay kinetics of the CL bands were obtained at an electron beam energy $U = 20$ keV, an absorbed current $I = 15$ nA, and a beam diameter $d = 2\,\mu$m. The CL spectra of the samples were recorded under the same conditions in the wavelength range $\lambda = 400-750$ nm, the decay kinetics were measured in the electron beam deflection mode also under the same conditions for all samples. CL images of the samples were obtained under the following conditions: electron beam energy $U = 20$ keV, absorbed current $I = 15$ nA, and beam diameter $d = 100\,\mu$m.

Results and discussion

Elemental composition of samples

The average elemental composition of the samples was determined by EPMA, the results are presented in Table 1. The obtained values of the elements content corresponded to the planned ones, the deviation from the planned composition does not exceed the error limits of the measurement method for all samples (10% for europium, 2% for other elements in the samples [11]).

Table 2. Asymmetry coefficient $\max I_{(ED)}/I_{(MD)}$ of the studied samples

Sample	$\max I_{(ED)}/I_{(MD)}$	Mean Deviation
0-Hf	1.33	0.08
0.41-Hf	1.4	0.02
0.62-Hf	1.41	0.02
0.82-Hf	1.46	0.04

CL images

All samples were imaged in an optical microscope and CL images. The optical images of all samples show a contrast associated with the surface topography. The dark areas in CL images match the contrast in optical images, suggesting that the contrast in CL images is also related to the surface topography of the samples. This conclusion is confirmed by the fact that, according to the EPMA data, the samples are homogeneous.

As an example, Fig. 1, *a* shows a CL image of a 0-Hf sample, Fig. 1, *b* — image of the same area of this sample in an optical microscope .

CL spectra

The measured CL spectra are shown in Fig. 2. The observed emission bands are interpreted on the basis of the paper by K. Binnemans [5], thanks to which it was determined that all luminescence bands are associated with transitions in the Eu^{3+} ion. In particular, transitions from the $^5D_1$ to $^7F_1$, from $^5D_2$ to $^7F_1$, and from $^5D_0$ to $^7F_{0,1,2,3,4}$ level were observed in the CL spectra of all samples. It can be seen that the content of hafnium does not affect the position and number of the observed bands. The analysis of the luminescence spectra confirmed that the ceramics were indeed stabilized in the cubic phase. This is evidenced by the absence of splitting of the transition band $^5D_0 - ^7F_2$ Eu^{3+} [8].

According to the method proposed in the paper [6], the asymmetry coefficient was calculated for all samples (Table 2). In this paper, it was shown that the asymmetry

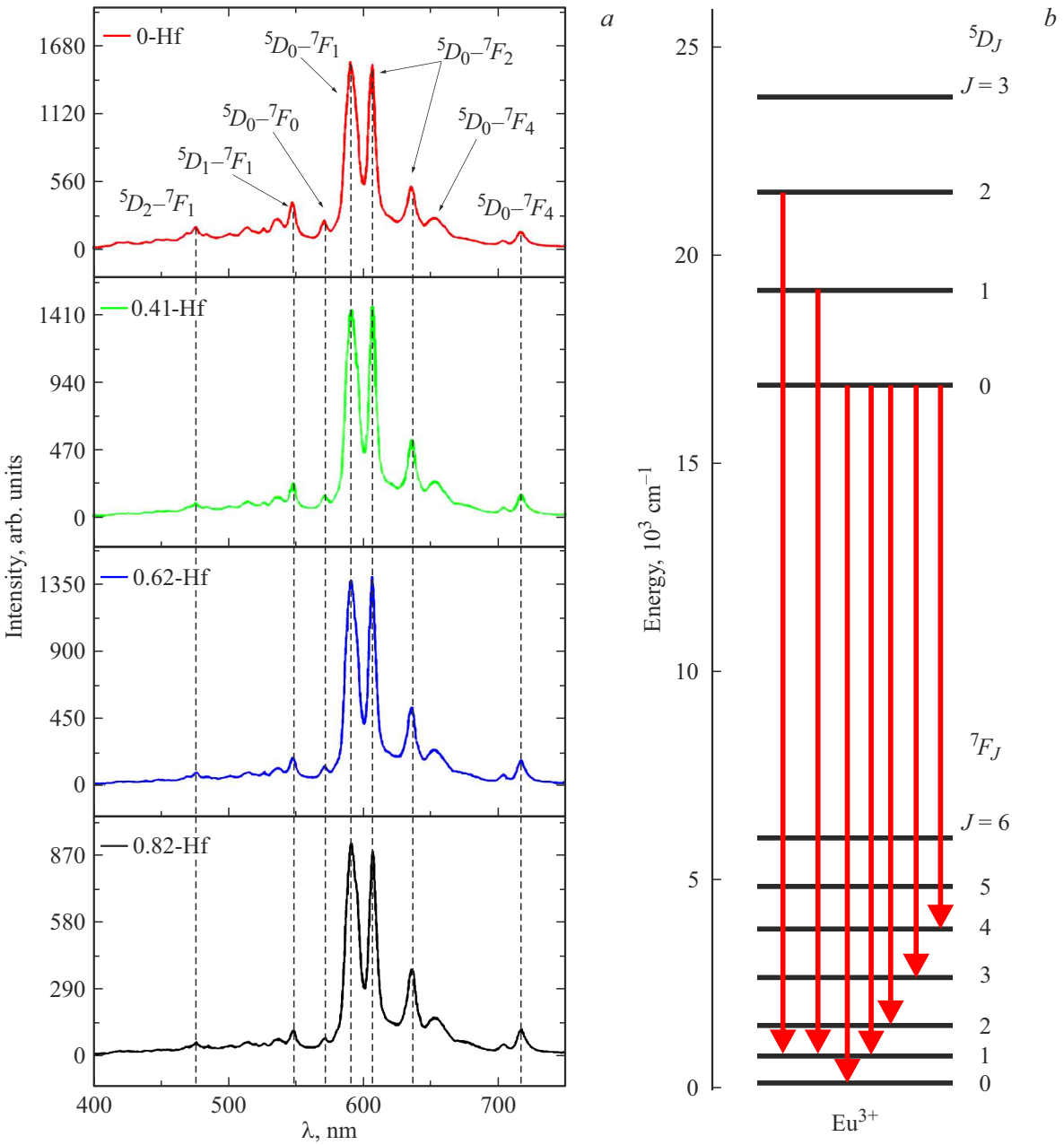

Figure 2. (*a*) CL samples spectra; (*b*) diagram of energy transitions of the europium ion in $(ZR_{0.82-x}HF_xY_{0.17}Eu_{0.01})O_{1.91}$.

coefficient $\max I_{(ED)}/I_{(MD)}$ (the ratio of the intensity maxima of the $^5D_0 - ^7F_1$ and $^5D_0 - ^7F_2$ bands) is very sensitive to changes in the local symmetry of the Eu^{3+}. ion.

The asymmetry factor $\max I_{(ED)}/I_{(MD)}$ is the ratio of the intensity maxima of the electric dipole transition $^5D_0 - ^7F_2$, which strongly depends on the environment of the activator ion, and the magnetic dipole transition $^5D_0 - ^7F_1$, which depends weakly on the environment. Comparing the $\max I_{(ED)}/I_{(MD)}$ concentration series of samples, the change in the local environment of the ion Eu^{3+} can be judged.

The results of the study show an increase in the asymmetry coefficient with an increase in the content of hafnium. This indicates a decrease in the symmetry of the europium environment with an increase in the hafnium content.

Study of the decay kinetics of the transition $^5D_0 - ^7F_1$ Eu^{3+}

In the course of the paper, the decay kinetics of the luminescence intensity of the $^5D_0 - ^7F_1$ ($\lambda = 590$ nm) transition of europium was also studied for all samples. The method of measuring the decay kinetics is described in the papers [11,12]. Kinetic dependences were obtained in different areas of the sample for each sample. An example

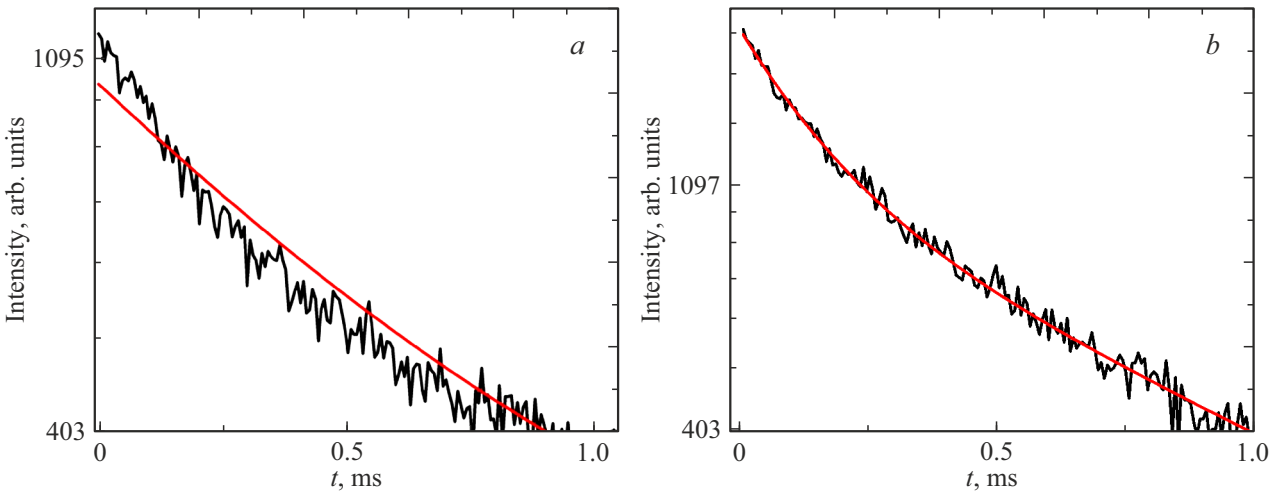

Figure 3. The CR intensity kinetics of the 0.41-Hf sample (black curve) on a semi-logarithmic scale, approximated by mono- (*a*) and bi-exponential functions (red curves) (*b*).

Table 3. Luminescence decay parameters for the transition $^5D_0 - ^7F_1$ Eu^{3+}

Pattern 0-Hf				Pattern 0.41-Hf			
Parameters number of the area	1	2	3		1	2	3
A_1	0.59	0.54	0.46	A_1	0.49	0.14	0.56
τ_1, ms	0.12	0.21	0.16	τ_1, ms	0.16	0.09	0.23
A_2	0.41	0.46	0.54	A_2	0.51	0.86	0.44
τ_2, ms	0.78	1.17	0.94	τ_2, ms	0.89	0.75	1.24
τ_{aver}, ms	0.66	1.00	0.84	τ_{aver}	0.78	0.74	1.04
Pattern 0.62-Hf				Pattern 0.82-Hf			
	1	2	3		1	2	3
A_1	0.50	0.53	0.55	A1	0.38	0.51	0.52
τ_1, ms	0.19	0.24	0.22	τ_1, ms	0.11	0.17	0.22
A_2	0.50	0.47	0.45	A_2	0.62	0.49	0.48
τ_2, ms	1.09	1.25	1.22	τ_2, ms	0.83	1.06	1.14
τ_{aver}, ms	0.96	1.07	1.04	τ_{aver}	0.78	0.93	0.98

of the dependence of the CR intensity on time is shown in Fig. 3, *b* on a semilogarithmic scale.

As can be seen in Fig. 3, *b*, this dependence cannot be approximated by a single exponent, therefore, each decay kinetics obtained for all samples was approximated by the sum of two exponents (1):

$$I = I_0 + A_1 \exp\left(-\frac{t}{\tau_1}\right) + A_2 \exp\left(-\frac{t}{\tau_2}\right). \qquad (1)$$

The presence of a shorter decay time may be due to the influence of the grain boundaries that make up the ceramic [4]. In case of describing the decay kinetics by a biexponential function, the average luminescence decay time τ_{aver} can be calculated, which is determined by the expression (2) [13]

$$\tau_{aver} = \frac{A_1 \cdot \tau_1^2 + A_2 \cdot \tau_2^2}{A_1 \cdot \tau_1 + A_2 \cdot \tau_2}. \qquad (2)$$

The results of approximation of the decay kinetics for the samples in different areas are presented in Table 3 (A_1, A_2 — contributions of the first and second exponents, respectively). The measurement error is 2% for τ_2 and 6% for τ_1.

It can be seen from the presented table that in each sample for different areas, both the value of the contribution of the exponent changes (for example, for 0-Hf A_1 it changes from 0.6 to 0.45) and the decay times. The short decay time changes especially strongly (up to 2 times). Also, for the entire concentration series of samples, the value of τ_{aver} varies from 0.66 to 1.07 ms. The τ_{aver} value does not correlate with the hafnium concentration.

It was demonstrated in the paper [12] that grain boundaries and interfaces make a significant contribution to the decay kinetics of rare-earth ions. Near the grain boundaries and interfaces, there are luminescence centers with a short decay time. Since the grain sizes in the studied ceramics are comparable with the size of the CR generation area (on the order of a few microns), the ratio of luminescent centers with long and short lifetimes can change significantly in different random areas, and, as a result, the contribution of the exponents and τ_{aver} changes.

Conclusions

In the paper, a series of ceramic samples with different hafnium content of the following composition was studied: $(Zr_{0.82-x}Hf_xY_{0.17}Eu_{0.01})O_{1.91}$ ($x = 0$, 0.41, 0.62 and 0.82).

It was shown that the CL image of the surface is heterogeneous. This is due to the features of the topography and sample preparation, and not to the heterogeneity of the

composition. In addition, when analyzing the spectra, it was shown that ceramic samples are represented by a cubic phase, an increase in the content of hafnium leads to a decrease in the local symmetry of europium. When studying the decay kinetics of the $^5D_0-^7F_1$ to Eu^{3+} transition, it was found that, due to the presence of ceramic grain boundaries and the formation of centers with a short decay time in random areas of the samples, the decay times and the contribution of the exponentials describing the kinetics of europium CL change strongly. The content of hafnium does not explicitly affect the decay times of europium CL and the contribution of the exponents describing long and shorter decay times.

Conflict of interest

The authors declare that they have no conflict of interest.

References

[1] S. Chand, R. Mehra, V. Chopra. V. Lumin., **36** (8), 1808 (2021). DOI:10.1002/bio.3960
[2] K. Yuan, X. Jin, Z. Yu, X. Gan, X. Wang, G. Zhang, L. Zhu, D. Xu, K. Yuan, X. Jin, Z. Yu, X. Gan, X. Wang, G. Zhang, L. Zhu, D. Xu. Ceram. Int., **44** (1), 282 (2018). DOI: 10.1016/j.ceramint.2017.09.171
[3] J. Dexpert-Ghys, M. Faucher, P. Caro. J. Solid State Chem., **54** (2), 179 (1984). DOI: 10.1016/0022-4596(84)90145-2
[4] H. Yu, C. Liu, Zh. Zhang, Sh. Huang, Y. Yang, R. Mao, He Feng, J. Zhao. Chem. Phys. Lett., 738 (2020). DOI: 10.1016/j.cplett.2019.136916
[5] K. Binnemans. Coord. Chem. Rev., **295**, 1 (2015). DOI: 10.1016/j.ccr.2015.02.015
[6] V.A. Kravets, K.N. Orekhova, M.A. Yagovkina, E.V. Ivanova, M.V. Zamoryanskaya. Opt. i spektr., **125** (2), 180 (2018) (in Russian). DOI: 10.61011/EOS.2023.05.56509.76-22
[7] K. Smits, L. Grigorjeva, D. Millers, A. Sarakovskis, A. Opalinska, J. D. Fidelus, W. Lojkowski. Opt. Mater., **32** (8), 827 (2010). DOI: 10.1016/j.optmat.2010.03.002
[8] E.V. Ivanova, V.A. Kravets, K.N. Orekhova, G.A. Gusev, T.B. Popova, M.A. Yagovkina, O.G. Bogdanova, B.E. Burakov, M.V. Zamoryanskaya. J. Alloys Compd., **808**, 151778 (2019). DOI: 10.1016/j.jallcom.2019.151778
[9] A.A. Shakirova, G.A. Gusev, E.V. Dement'eva, A.A. Averin, T.B. Popova, M.V. Zamoryanskaya. Opt. i spectr., **130**, 10 (2022). (in Russian) DOI: 10.61011/EOS.2023.05.56509.76-22
[10] M.V. Zamoryanskaya, S.G. Konnikov, A.N. Zamoryanskii. Instrum. Exp. Tech., **47** (4), 447 (2004). DOI: 10.1023/B:INET.0000038392.08043.d6
[11] G.A. Gusev, S.M. Masloboeva, M.A. Yagovkina, M.V. Zamoryanskaya. Opt. i spektr., **130** (2), 294 (2022) (in Russian). DOI: 10.61011/EOS.2023.05.56509.76-22
[12] K. Orekhova, M. Zamoryanskaya. J. Lumin., **251**, 119228 (2022).
[13] I.E. Kolesnikov, D.S. Kolokolov, M.A. Kurochkin, M.A. Voznesenskiy, M.G. Osmolowsky, E. Lähderanta, O.M. Osmolovskaya. J. Alloys Compd., **822**, 153640 (2020). DOI: 10.1016/j.jallcom.2020.153640

Translated by E.Potapova